Structural Engineering and Mechanics, Vol. 29, No. 2 (2008) 117-134
DOI: http://dx.doi.org/10.12989/sem.2008.29.2.117

Dynamic analysis of 3-D structures with adaptivity in RBF of dual reciprocity BEM

S.H. Razaee† and A. Noorzad‡

Department of Civil Engineering, Engineering Faculty, Tehran University, Tehran, Iran

(Received December 2, 2005, Accepeted March 7, 2008)

Abstract. A new adaptive dual reciprocity boundary element method for dynamic analysis of 3-D structures is presented in this paper .It is based on finding the best approximation function of a radial basis function (RBF) group $f = r^n + c$ which minimize the error of displacement field expansion. Also, the effects of some parameters such as the existence of internal points, number of RBF functions and position of collocation nodes in discontinuous elements are investigated in this adaptive procedure. Three numerical examples show improvement in dynamic response of structures with adaptive RBF in dual reciprocity with respect to ordinary BEM.

Keywords: Adaptive Dual Reciprocity; Boundary Element; Radial Basis Functions (RBF); natural frequencies; collocation node.

1. Introduction

The Boundary Element Method (BEM) is a powerful numerical method for structural analysis. The BEM as applied to elastodynamic analysis in the frequency or time domain, usually employs the corresponding elastodynamic fundamental solution.

However, the use of the elastodynamic fundamental solution increases the computational effort due to large computation of convolution integral in forced vibration analysis and in addition creates problems of accuracy and efficiency in free vibration analysis, where eigenvalues are computed by the inefficient method of determinant.

Nardini and Brebbia (1982) introduced the Dual Reciprocity Boundary Element Method (DR/BEM) in which much simpler elastostatic fundamental solution is used. For dynamic analysis, this method creates an inertial volume integral due to acceleration term. The volume integral is transformed into a surface integral with the aid of the reciprocal theorem. Thus, they succeeded in creating a BEM which combines the dimensionality reduction advantage with the simplicity of the elastostatic fundamental solutions. The 3-D DR/BEM has been applied by Wang and Banerjee (1988, 1990) and Wilson *et al.* (1990) to free vibration analysis of axisymmetric structures. However, no extensive studies concerning the influence of the selected approximation function on the obtained results have been provided in their works. A development has been made by Agnantiaris, Polyzos and Beskos (1998, 2001) for implementation of DR/BEM to three-dimensional

† Ph.D. Student, Corresponding author, E-mail: shrezaee@ut.ac.ir, shrazaee@yahoo.com
‡ Assistant Professor, E-mail: noorzad@ut.ac.ir

(3-D) elastodynamic analysis including both free and forced vibration problems. Later, they used some local radial basis functions (RBFs) with or without augmentation to free vibration analysis of non-axisymmetric and axisymmetric structures. Also, Golberg *et al.* (1996, 1998) performed some researches on the use of various approximation functions such as mutiquadraticlocal RBF $(\sqrt{r^2+c^2})$ and effect of augmentation term in thin plate spline RBF $(r^2 \ln r)$.

This paper presents an adaptive procedure in a group of local RBF $f = r^n + c$ for best selection of it's parameters.

As the dynamic analysis in BEM depends on important factors such as internal points number, parametric position of collocation nodes in discontinuous elements and RBFs number (geometrical boundary points number), the effects of these factors in the adaptive procedure are discussed in third section. After finding the best parameters of the problem, dynamic analysis with DR/BEM can be performed more accurate than ordinary procedure of DR/BEM.

Three numerical examples of a cube, beam and sphere are presented in fourth section. The accuracy of natural frequencies, response amplitude of harmonic forced vibration in frequency domain and displacements time history of transient loading in time domain show the efficiency of presented method.

2. The DR/BEM Formulation in elastodynamics

The motion of a linearly elastic body of domain Ω and boundary Γ is described by the Navier-Cauchy partial differential equation as

$$\mu \Delta_x \mathbf{u}(\mathbf{x},t) + (\lambda+\mu)\nabla_x \nabla_x \mathbf{u}(\mathbf{x},t) = \rho \ddot{\mathbf{u}}(\mathbf{x},t) \tag{1}$$

Where $\mathbf{u}(\mathbf{x},t)$ is the displacement vector at point $\mathbf{x}$ and time t, λ and μ being the Lame elastic constants and ρ the mass density. Assuming zero body forces and zero initial conditions, the integral representation of the Eq. (1) is formed as

$$c(\mathbf{x})u_i(\mathbf{x},t) = \int_\Gamma [G_{ij}(\mathbf{x},\zeta)\phi_j(\zeta,t) - F_{ij}(\mathbf{x},\zeta)u_j(\zeta,t)]\mathrm{d}\Gamma(\zeta) - \int_\Omega G_{ij}(\mathbf{x},\zeta)\rho\ddot{u}_j(\zeta,t)\mathrm{d}\Omega(\zeta) \tag{2}$$

Where $c(\mathbf{x})$ is the jump tensor. $G_{ij}(\mathbf{x},\zeta)$ and $F_{ij}(\mathbf{x},\zeta)$ are the fundamental solutions of displacement and traction tensors in static problems. $u_i(\mathbf{x},t)$ and $\phi_j(\zeta,t)$ are the displacement and traction vectors at point ζ. The unknown solution $\mathbf{u}(\mathbf{x},t)$ is expressed inside Ω as a series of unknown time dependent coefficients $\alpha_i^m(t)$ and known basis functions $f^m(x)$ of the form

$$u_i(\mathbf{x},t) = \sum_{m=1}^{M} \alpha_i^m(t) f^m(\mathbf{x}) \tag{3}$$

Where M is RBF number, which equal to the number of selected geometrical boundary points. It is common to use RBFs because of their simplicity

$$f^m(\mathbf{x}) = f(r(\mathbf{x}, \zeta^m)) \tag{4}$$

Where r is the Euclidean distance from point x to point ζ^m. Inserting expression (3) into the domain integral of Eq. (2) and reusing the reciprocity principle, the domain integral transforms into a

boundary integral

$$-\int_{\Omega} G_{ij}(\mathbf{x},\zeta)\rho\ddot{u}_j(\zeta,t)\mathrm{d}\Omega(\zeta) =$$
$$\rho\sum_{m=1}^{M}\ddot{\alpha}_n^m(t)[C_{ij}(\mathbf{x})\psi_{jn}^m(\mathbf{x}) + \int_{\Gamma}[F_{ij}(\mathbf{x},\zeta)\psi_{jn}^m(\mathbf{x}) - G_{ij}(\mathbf{x},\zeta)\eta_{jn}^m(\mathbf{x})]\mathrm{d}\Gamma(\zeta)] \tag{5}$$

Where $\psi_{jn}^m(\mathbf{x})$ is the particular solution (displacement) of the Navier-Cauchy partial differential equation and $\eta_{jn}^m(\mathbf{x})$ is the corresponding traction field. For the presented RBF, $f = r^n + c$ these functions are

$$\psi_{ij}^m = \frac{1}{4\mu(1-\nu)}\left[(3-4\nu)\left(\frac{1}{(n+2)(n+3)}r^{n+2} + \frac{c}{6}r^2\right) + \frac{1}{(n+2)(n+5)}r^{n+2} + \frac{c}{10}r^2\right]\delta_{ij}$$
$$-\frac{1}{4\mu(1-\nu)}\left(\frac{2}{(n+3)(n+5)}r^n + \frac{2c}{15}\right)r_i r_j \tag{6}$$

and

$$\eta_{ij}^m = \frac{1}{2(1-\nu)}\left[(1-2\nu)\left(\frac{c}{3} + \frac{1}{n+3}r\right) + \frac{c}{5} + \frac{1}{n+5}r\right](r_i n_j + r_k n_k \delta_{ij})$$
$$-\frac{1}{2(1-\nu)}\left[(1-2\nu)\left(\frac{c}{3} + \frac{1}{n+3}r\right) - \left(\frac{c}{5} + \frac{1}{n+5}r\right)\right]r_j n_i$$
$$-\frac{1}{2(1-\nu)}\frac{2n}{(n+3)(n+5)}r^{n-2}r_i r_j r_k n_k \tag{7}$$

Discretizing of the boundary Γ into a finite number of boundary elements with a total number of N nodes and rewriting of Eq. (2) in conjunction with Eq. (5) for all these nodes, the matrix equation is obtained as

$$[F]\{U\} = [G]\{\Phi\} + \rho([F][\psi] - [G][\eta])\{\ddot{\alpha}\} \tag{8}$$

Where $[F]$ and $[G]$ are the elastostatic influence matrices, $\{U\}$ and $\{\phi\}$ are the boundary displacement and traction vectors, respectively. $[\psi]$ and $[\eta]$ are matrices containing sub-matrices of ψ_j^m and η_j^m types. These sub-matrices correspond to the m-order radial function and each row to the j nodal point. Applying expansion (3) to all geometrical boundary points M and assembling of the resulting equations produces

$$\{\ddot{U}\} = [F_B]\{\ddot{\alpha}\} \tag{9}$$

Eq. (8) can be rewrite as follows

$$[H]\{\ddot{U}\} + [F]\{U\} = [G]\{\Phi\} \tag{10}$$

where

$$[H] = \rho([F][\Psi] - [G][\eta])[F_B]^{-1} \tag{11a}$$

It should be noted that if $M<N+L$ where L is the number of internal points, Eq. (11a) should be modified as

$$[H] = \rho([F][\Psi] - [G][\eta])[F_B^T \cdot F_B]^{-1}[F_B^T] \tag{11b}$$

The above equation can be used in frequency domain by considering time harmonic dependent boundary displacement and traction vectors. This leads to

$$(-\omega^2[H] + [F])\{\tilde{U}\} = [G]\{\tilde{\Phi}\} \tag{12}$$

where ω is the circular frequency of the harmonic excitation. For calculation of natural modes and frequencies, Eq. (12) is used by setting the external disturbances equal to zero. This results to a generalized algebraic eigenvalue problem represented by the equation

$$[A]\{x\} = \omega^2[H^*]\{x\} \tag{13}$$

where $[A]$ is the BEM influence matrix created from moving the columns of $[G]$ corresponding to all unknown boundary variables to $[F]$. $[H^*]$ is obtained from $[H]$ by putting zeros in its sub-columns related to known displacements.

It should be noted that matrices $[A]$ and $[H^*]$ are both fully populated and non-symmetric. For solving the generalized algebraic eigenvalue problem of Eq. (13), an appropriate algorithm should be selected.

3. Adaptivity in RBF of dual reciprocity

The general errors in the BEM can be divided into the following four categories (Zhao and Wang 1999):

(a) Idealization error: This error is due to the transformation from the physical problem into a mathematical model.

(b) Implementation error: This error refers to the numerical schemes used to implement the boundary integral equation, e.g., the numerical scheme to compute various integrals, equation solver, etc. Because of the singular and the nearly singular integrals involved, the implementation error should be dealt carefully. Although the BEM implementation has been improved by using advanced integral schemes, the implementation error is still an important factor to the success of the BEM analyses.

(c) Round-off and precision error: This error results from repeating computation, and can be kept at a lower level by careful programming and by using higher precision.

(d) Discretization error: This error in the BEM analyses includes the geometric discretization error. Adaptive methods such as h, P, r and their combinations concern with this type of error.

There is another error in Dual Reciprocity BEM of approximating the displacement field with approximating functions which is presented in Eq. (3). The effect of this error appears in calculation of $[H]$ in Eq. (11a) or (11b). A group of RBF that covers suitable local RBFs such as $r+1$, r, r^3, r^3+1 in 3-D application of DR/BEM is $f = r^n + c$ with major parameter of 'n' and augmentation parameter of 'c'. It should be noted that 'n' is real positive number but 'c' has no restriction. The

effect of augmentation parameter 'c' has been tested for the three presented examples and its effect is negligible. This is the fact that also mentioned by Prtridge (2000) and Agnantiaris (2001) for the effect of augmentation term in radial basis functions. Thus, in adaptive RBF scheme the concentration will be on 'n' exponent.

Based on Eq. (13), $[B]$ is introduced as

$$[B] = [A]^{-1}[H^*] \tag{14}$$

The eigenvalues of $[B]$ are inverse square of the problem's natural frequencies. As, the accuracy any dynamic analysis directly relates to accuracy of $[B]$ elements, the error estimator is introduced in L_2 norm

$$\varepsilon = sqrt\left(\sum_{i=1}^{ND}\sum_{j=1}^{ND}(B'_{ij} - B''_{ij})^2\right) \tag{15}$$

Where ND is the dimension of $[B]$, B'_{ij} and B''_{ij} are elements of $[B]$ corresponding to RBFs of $f = r^{n'}$ and $f = r^{n''}$.

The RBF adaptivity is based on the minimization of ε in sequence of 'n' and derivation of $n_{opt.}$. In this paper, searching for $n_{opt.}$ is limited to the interval $0.0 < n < 4.0$ that seems to be enough.

The following steps should be considered for implementation of RBF adaptivity:

1- Assignment of suitable RBFs number (M)

The RBFs number is one of the important parameters in DR/BEM used in displacement field expansion. They should be well distributed for better description of the geometry. The RBFs number usually is equal to all geometrical boundary points' number but it is possible to use a selection of them which are more important in problem's geometrical description.

2- Assignment of parametric position of collocation nodes (λ) in discontinuous elements (Fig. 1)

3- Minimization of ε in sequence of 'n' and derivation of $n_{opt.}$

4- Assignment of internal points (I.P.)

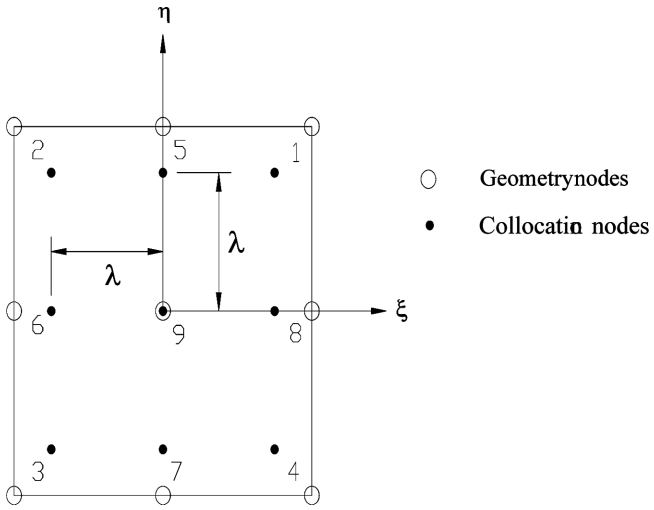

Fig. 1 Quadrilateral discontinuous element

Internal points may improve the accuracy of the analysis in some problems especially in case of coarse meshes. They should be distributed in the structure as uniformly as possible.

For checking the efficiency of the method, the results of natural frequencies are compared with references.

4. Numerical Examples

Example. 1- An elastic solid cube of side $L = 6$ (m) with bottom fixed face is solved by the RBF adaptivity in DR/BEM method. The material properties are as follows:

Shear modulus $\mu = 10^6$ (Pa),

Poisson's ratio $\nu = 0.3$,

Mass density $\rho = 100$ (Kg/ m^3)

The cube is discretized with nine-node-quadratic-quadrilateral discontinuous elements (Fig. 1) to 24 elements (Fig. 2a). This kind of elements is used in order to accommodate the corner and edge effects. The eigenfrequencies of the cantilever cube are normalized with the expression $\omega^* = \omega L\sqrt{\rho/E}$ where E is elasticity modulus.

RBFs number is equal to $M = 98$ f based on usage of all geometrical nodes.

As shown in Table 1(a), the results of first eight natural frequencies of the cube with other fixed parameters show that $M = 98$ has the minimum errors between other geometrical boundary point numbers.

In second step, $\lambda = 0.50, 0.60, 0.67, 0.75, 0.80, 0.83, 0.90$ are tested and the results are shown in Table 1(b). The results of first eight natural frequencies of the cube with other fixed parameters show that all above tested ratios are acceptable but $\lambda = 0.83$ is the best selection for this problem.

With above selected parameters the specification of the RBF $f = r^n$ for $0.0 < n < 4.0$ are as follows:

The result of RBF adaptivity (Fig. 3) shows that the interval of $0.5 < n < 1.1$ produce agreeable results and $n_{opt.}$ is equal to 0.8. Checking the adaptivity results, the errors of first eight natural frequencies are derived (Figs. 4a-f) based on analytic results calculated by Leissa and Zhang (1983). They showed that each mode has own $n_{opt.}$ but $n = 0.8$ has acceptable errors in all first eight modes.

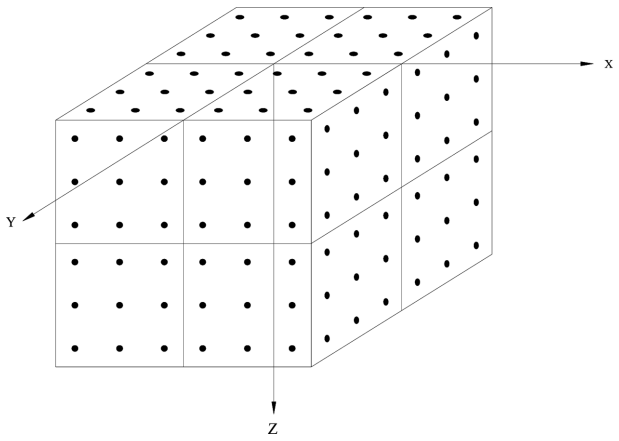

Fig. 2(a) Cube surface discritization to 24 quadrilateral discontinuous elements

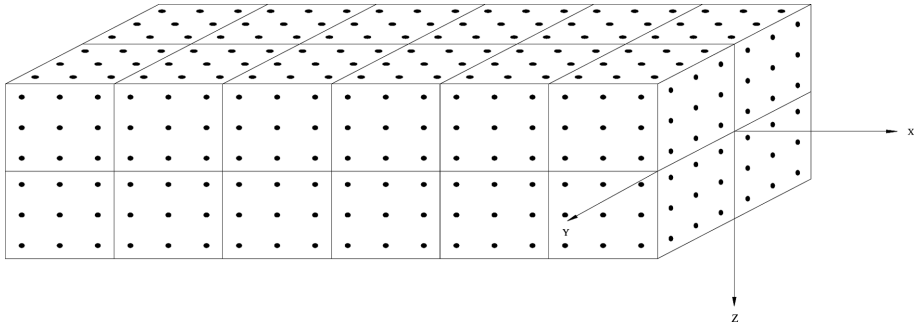

Fig. 2(b) Beam surface discritization to 56 quadrilateral discontinuous elements

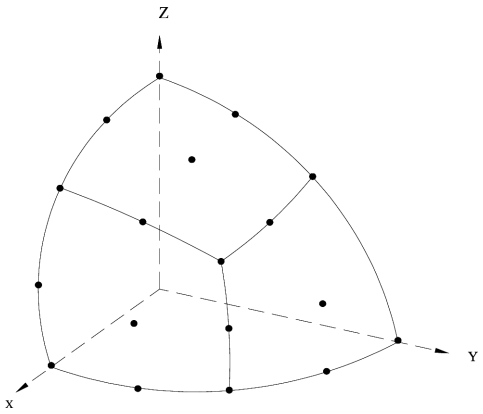

Fig. 2(c) Sphere surface discritization to 24 quadrilateral elements

Table 1(a) Normalized eigenfrequencies of the cantilever cube (24El., $\lambda = 0.67$, $f = 1 + r$, I.P. = 0)

Mode	ω_i^* (Type)	($M = 26$) $\hat{\omega}_i^*$ e_i (%)	($M = 98$) $\hat{\omega}_i^*$ e_i (%)	($M = 152$) $\hat{\omega}_i^*$ e_i (%)
1, 2	0.670 (Bending)	0.664 (0.84)	0.665 (0.77)	0.665 (0.75)
3	0.909 (Torsion)	0.896 (1.47)	0.902 (0.81)	0.902 (0.76)
4	1.599 (Longitudinal)	1.601 (0.13)	1.597 (0.10)	1.596 (0.16)
5, 6	1.769 (Bending)	1.766 (0.18)	1.755 (0.82)	1.755 (0.81)
7	2.180 (Torsion)	2.232 (2.38)	2.167 (0.62)	2.162 (0.84)
8	2.581 (Longitudinal)	2.559 (0.87)	2.517 (2.48)	2.516 (2.52)

The last step is decision about internal point's number and locations. In three cases of internal points I.P. = 0, 8, 27, the results are presented in each mode (Table 1(c)).

Table 1(b) Normalized eigenfrequencies of the cantilever cube (24El., $M = 98$, $f = 1 + r$, I.P. = 0)

Mode	ω_i^* (Type)	($\lambda = 0.50$) $\hat{\omega}_i^*$ e_i (%)	($\lambda = 0.60$) $\hat{\omega}_i^*$ e_i (%)	($\lambda = 0.67$) $\hat{\omega}_i^*$ e_i (%)	($\lambda = 0.75$) $\hat{\omega}_i^*$ e_i (%)	($\lambda = 0.80$) $\hat{\omega}_i^*$ e_i (%)	($\lambda = 0.83$) $\hat{\omega}_i^*$ e_i (%)	($\lambda = 0.90$) $\hat{\omega}_i^*$ e_i (%)
1, 2	0.670 (Bending)	0.659 (1.57)	0.660 (1.44)	0.665 (0.77)	0.665 (0.81)	0.669 (0.13)	0.671 (0.10)	0.674 (0.66)
3	0.909 (Torsion)	0.895 (1.58)	0.895 (1.59)	0.902 (0.81)	0.900 (1.04)	0.905 (0.39)	0.907 (0.23)	0.910 (0.15)
4	1.599 (Longitudinal)	1.595 (0.25)	1.601 (0.12)	1.597 (0.10)	1.601 (0.12)	1.602 (0.16)	1.603 (0.27)	1.609 (0.61)
5, 6	1.769 (Bending)	1.745 (1.37)	1.757 (0.66)	1.755 (0.82)	1.762 (0.37)	1.764 (0.26)	1.767 (0.10)	1.773 (0.21)
7	2.180 (Torsion)	2.166 (0.64)	2.168 (0.55)	2.167 (0.62)	2.173 (0.31)	2.173 (0.33)	2.175 (0.24)	2.180 (0.00)
8	2.581 (Longitudinal)	2.508 (2.83)	2.527 (2.11)	2.517 (2.48)	2.527 (2.11)	2.533 (1.85)	2.538 (1.68)	2.545 (1.39)

Table 1(c) Normalized eigenfrequencies of the cantilever cube (24El., $\lambda = 0.83$, $f = r^{0.8}$, $M = 98$)

Mode	ω_i^* (Type)	(I.P = 0) $\hat{\omega}_i^*$ e_i (%)	(I.P = 8) $\hat{\omega}_i^*$ e_i (%)	(I.P = 27) $\hat{\omega}_i^*$ e_i (%)
1, 2	0.670 (Bending)	0.670 (0.00)	0.670 (0.00)	0.670 (0.00)
3	0.909 (Torsion)	0.905 (0.44)	0.906 (0.33)	0.907 (0.21)
4	1.599 (Longitudinal)	1.612 (0.82)	1.608 (0.55)	1.602 (0.19)
5, 6	1.769 (Bending)	1.785 (0.92)	1.779 (0.56)	1.769 (0.00)
7	2.180 (Torsion)	2.194 (0.66)	2.190 (0.46)	2.185 (0.24)
8	2.581 (Longitudinal)	2.568 (0.52)	2.568 (0.51)	2.570 (0.45)

In this example, 8 internal points are the corners of a cube with side 4 (m) in the main cube and 27 internal points are located on the similar cube adding the center of each face and center of the whole cube. Comparing the differences between three cases results, I.P = 27 can be selected. As shown in Table 1(c), using 27 internal points improves the accuracy of cube's eigenfrequencies in modes 3-7.

Using the results of the RBF adaptive procedure, dynamic analysis can be done. For the first loading case, the cube is subjected to a uniform harmonically varying with time normal tensile traction of amplitude $P_0 = 100$ (Pa) acting on the cantilever cube on the top face. The amplitude of the harmonic displacement Uz at the middle point of the loaded face is plotted versus angular frequency (Fig. 5a). The results of the RBF adaptive DR/BEM are shown to be in close agreement with those obtained by Agnantiaris specially in low frequencies but the adaptive procedure have more accuracy specially in mode 4 which is main mode of resonance.

Table 1(d) Comparison of adaptive BEM results with ordinary BEM for cantilever cube (24El., I.P = 27)

Mode	ω_i^* (Type)	(Ordinary BEM) (Agnantiaris *et al.* (1998)) ($f = r + 1$) $\hat{\omega}_i^*$ e_i (%)	(RBF Adaptive BEM) ($f = r^{0.8}$) $\hat{\omega}_i^*$ e_i (%)
1, 2	0.670 (Bending)	0.670 (0.00)	0.670 (0.00)
3	0.909 (Torsion)	0.933 (2.64)	0.907 (0.21)
4	1.599 (Longitudinal)	1.602 (0.18)	1.602 (0.18)
5, 6	1.769 (Bending)	1.773 (0.22)	1.769 (0.00)
7	2.180 (Torsion)	2.156 (1.10)	2.185 (0.24)
8	2.581 (Longitudinal)	2.556 (0.96)	2.570 (0.45)

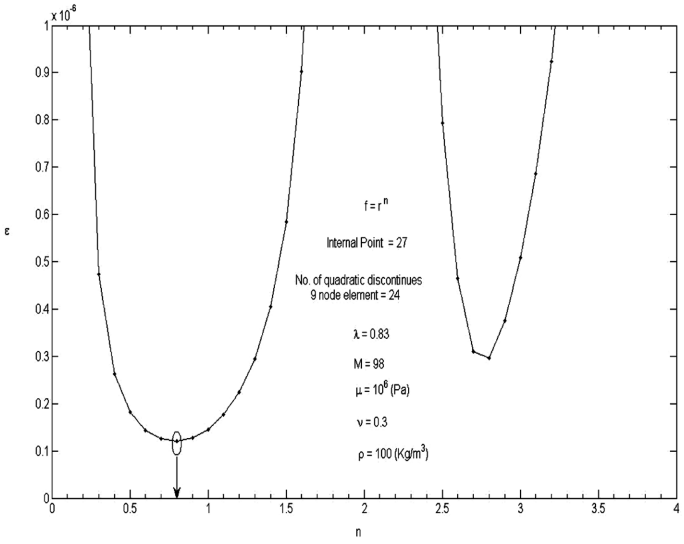

Fig. 3 Adaptive n selection in radial basis function $f = r^n$ for the cantilever cube

Finally the cube is subjected to a suddenly applied uniform tensile traction $P = P_0H(t)$ acting on the top face, where $P0 = 100$ (Pa) and $H(t)$ is the Heaviside function. The time history of the Uz displacement at the middle point of the loaded surface is compared with that obtained by Agnantiaris (Fig. 5b). The time step used in Houbolt's time integration scheme equals to $\Delta t = 0.01$ (s). This corresponds to $\beta = 0.75$ with definition of $\beta = C_P\Delta t/L$. In this expression, C_P and L are the longitudinal wave velocity of the elastic medium and the length between the nearest surface nodes, respectively. The results of the RBF adaptive DR/BEM are shown to be in close agreement with Agnantiaris *et al*. result. It worth noting that peak value should be two times of static displacement

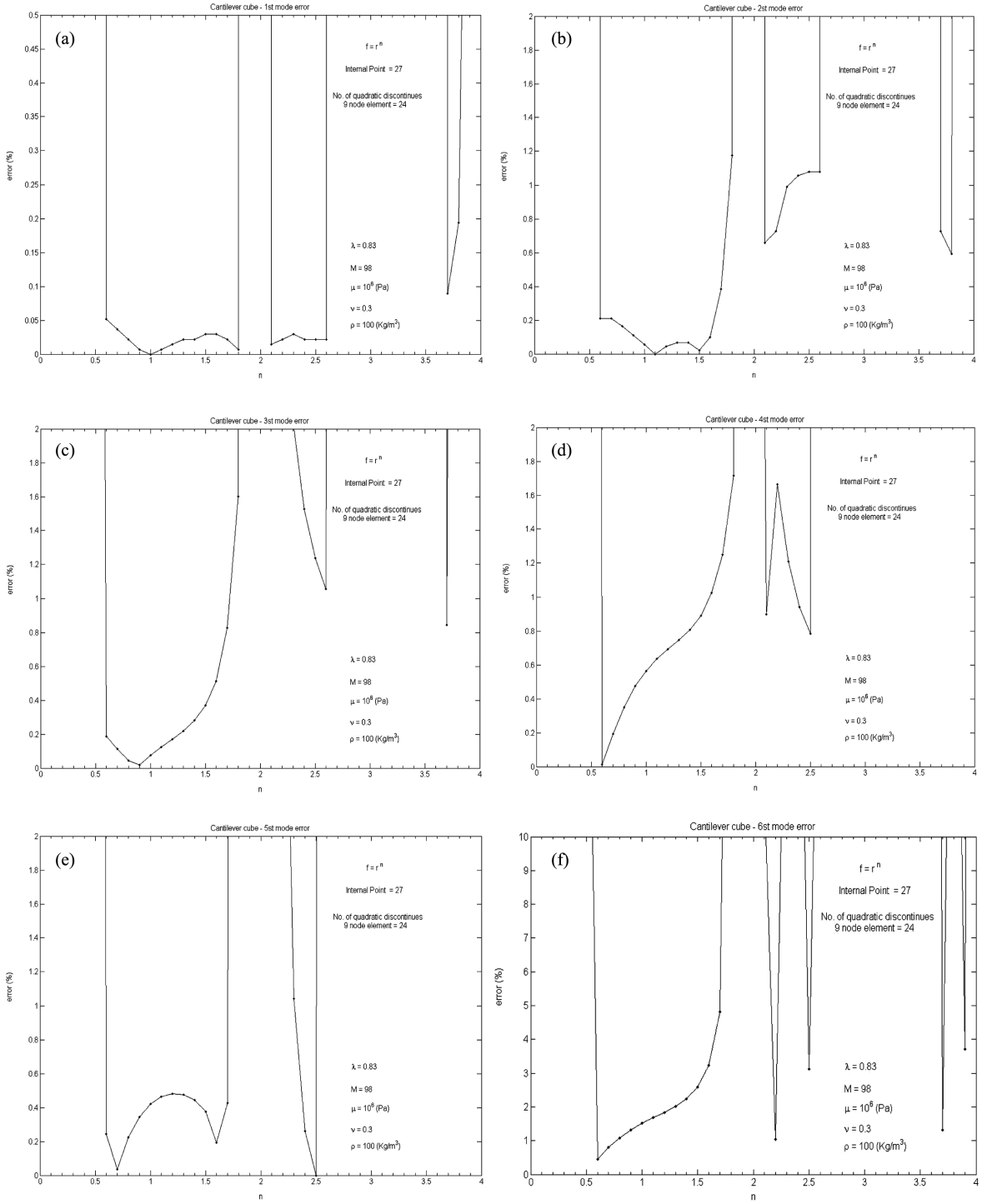

Fig. 4(a)-(f) Eigenfrequencies error of the cantilever cube

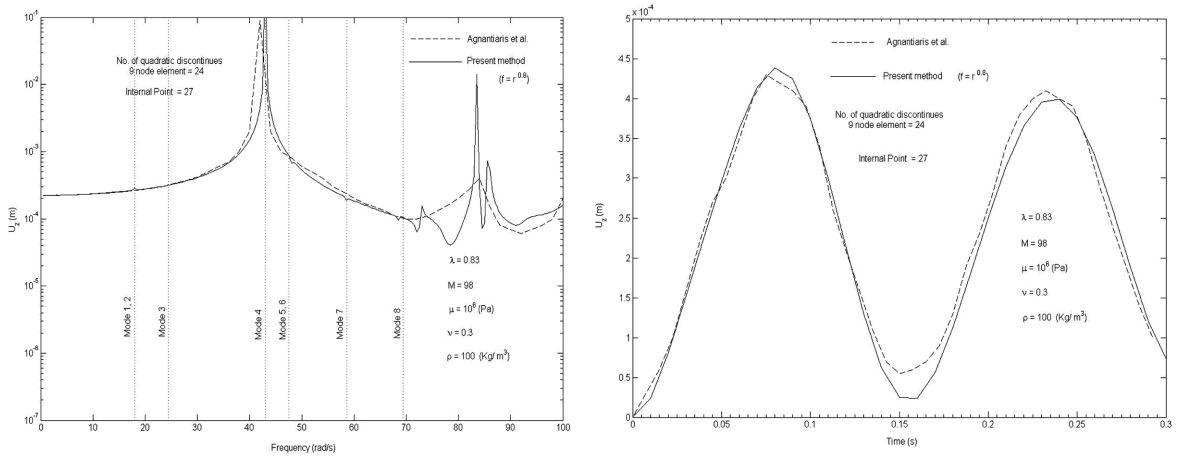

(a) (b)

Fig. 5(a),(b) Amplitude/Time History of the displacement at the mid-node of the loaded surface of the cube

about $U_{z,stat}$ = 2.24e-3 (m) and dip value should be zero because no damping is considered in the problem. Comparing the results shows that the adaptive procedure has more accuracy in peak and dip values.

Example. 2- An elastic cantilever beam of length L = 20 (m) with 4 (m) × 4 (m) cross section is solved by the RBF adaptive DR/BEM. The fixed base of the beam is subjected to a harmonic unit transversal motion. The material properties are as follows:

Shear modulus $\mu = 0.8 \times 10^{11}$ (Pa),

Poisson's ratio $\nu = 0.3$,

Mass density ρ = 7800 (Kg/m^3)

The beam surface is discretized to totally 56 nine-node-quadratic-quadrilateral-discontinuous elements with 48 elements for lateral faces and 4 elements for each beam end (Fig. 2b).

RBFs number is equal to M = 226 based on usage of all geometrical nodes. As shown in Table 2(a), the results of first six natural frequencies of the beam with other fixed parameters of λ = 0.83, $f = r^3$, I.P. = 0 shows that M = 226 has the minimum errors between other geometrical

Table 2(a) Eigenfrequencies of the cantilever beam (λ = 0.83, $f = r^3$, I.P. = 0)

Mode	ω_i^* (rad/s) (Type)	(M = 90) $\hat{\omega}_i^*$ e_i (%)	(M = 226) $\hat{\omega}_i^*$ e_i (%)
1, 2	51.48 (Bending)	54.0 (4.89)	54.0 (4.89)
3	233.04 (Torsion)	280.0 (20.15)	278.3 (19.42)
4,5	277.86 (Bending)	297.8 (7.18)	298.9 (7.59)
6	408.25 (Longitudinal)	404.1 (1.02)	404.3 (0.97)

Table 2(b) Eigenfrequencies of the cantilever beam ($M = 226$, $f = r^{1.4}$, I.P. = 0)

Mode	ω_i^* (rad/s) (Type)	($\lambda = 0.60$) $\hat{\omega}_i^*$ e_i (%)	($\lambda = 0.67$) $\hat{\omega}_i^*$ e_i (%)	($\lambda = 0.75$) $\hat{\omega}_i^*$ e_i (%)	($\lambda = 0.83$) $\hat{\omega}_i^*$ e_i (%)
1, 2	51.48 (Bending)	49.1 (4.62)	53.0 (2.95)	49.3 (4.14)	- (100.00)
3	233.04 (Torsion)	219.7 (5.72)	288.0 (23.58)	258.3 (10.84)	303.8 (30.36)
4,5	277.86 (Bending)	269.2 (3.12)	275.1 (0.99)	270.1 (2.81)	278.0 (0.05)
6	408.25 (Longitudinal)	406.6 (0.40)	406.4 (0.45)	406.8 (0.35)	406.6 (0.40)

Table 2(c) Eigenfrequencies of the cantilever beam ($M = 226$, $f = r^{2.7}$, $\lambda = 0.60$)

Mode	ω_i^* (rad/s) (Type)	(I.P. = 0) $\hat{\omega}_i^*$ e_i (%)	(I.P. = 9) $\hat{\omega}_i^*$ e_i (%)
1, 2	51.48 (Bending)	49.1 (4.62)	49.0 (4.92)
3	233.04 (Torsion)	220.0 (5.60)	219.7 (5.72)
4,5	277.86 (Bending)	270.7 (2.56)	- (100)
6	408.25 (Longitudinal)	405.6 (0.65)	- (100)

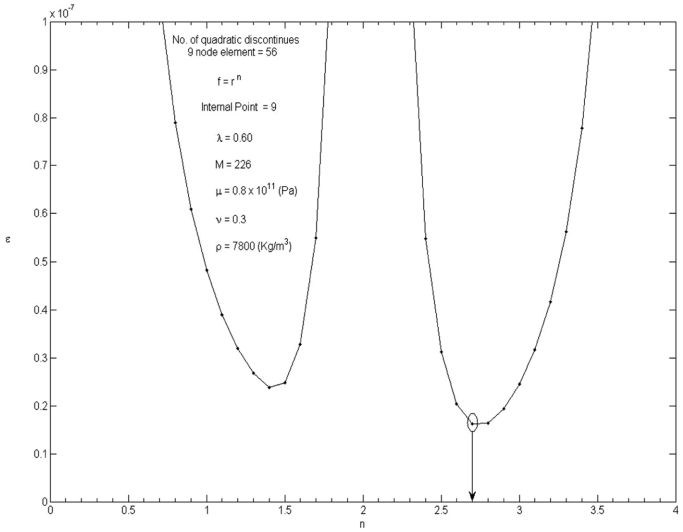

Fig. 6 Adaptive n selection in radial basis function $f = r^n$ for the cantilever beam

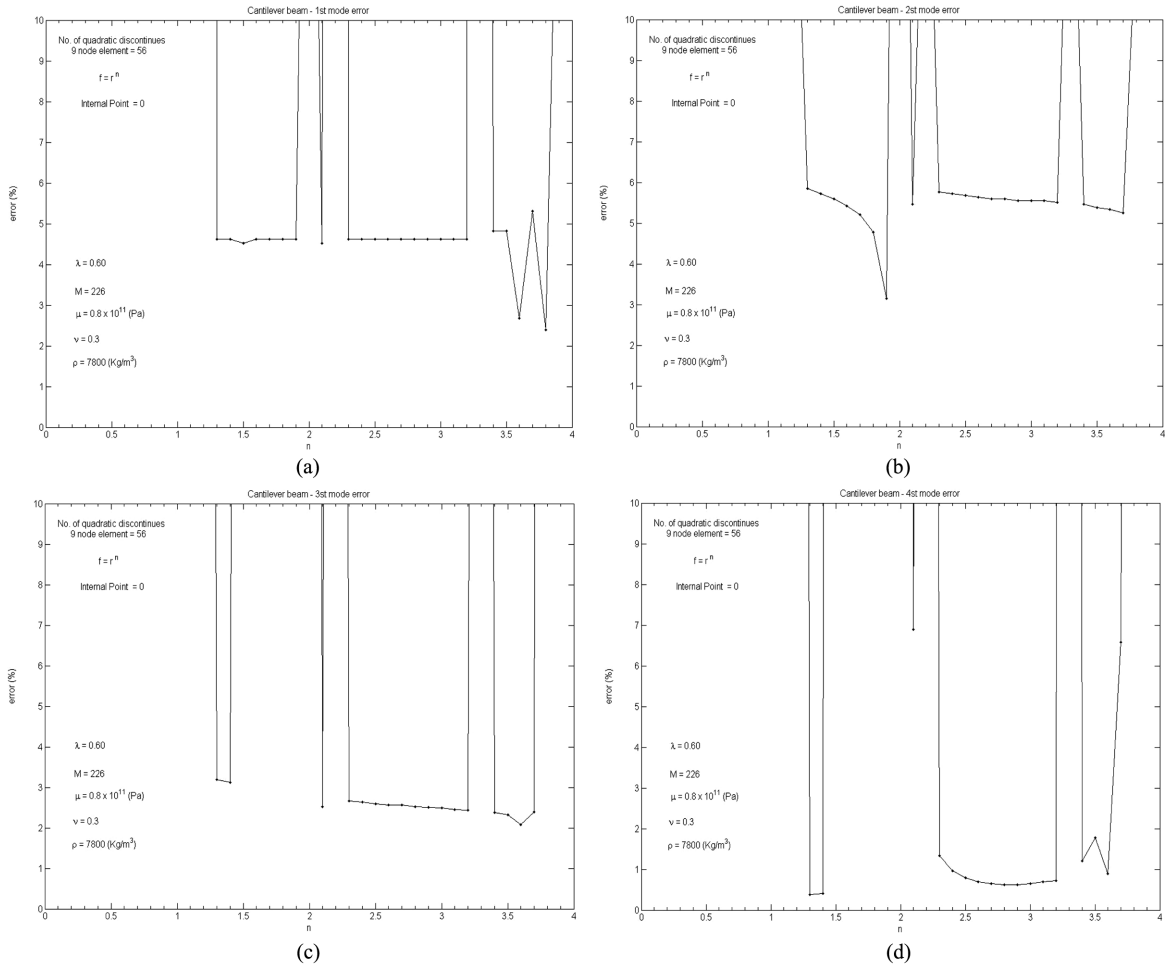

Fig. 7(a)-(d) Eigenfrequencies error of the cantilever beam

boundary point numbers.

In second step, λ = 0.60, 0.67, 0.75, 0.83, are tested and the results are shown in Table 2(b). In this table, the results of first six natural frequencies of the beam with other fixed parameters of M = 226, $f = r^{1.4}$, Int. point = 0 shows that λ = 0.60, 0.67, 0.75 are acceptable but λ = 0.60 is the best selection.

With λ = 0.60 and M = 226 the specification of the RBF $f = r^n$ for $0 < n < 4.0$ are as follows:

The result of RBF adaptivity (Fig. 6) shows that the interval of $2.5 < n < 3.1$ produce agreeable results and $n_{opt.}$ is equal to 2.7. Checking the adaptivity results, the errors of first six natural frequencies are derived (Figs. 7a-d) based on FEM results. It shows that each mode has own n_{opt} but n = 2.7 have acceptable errors in all first six modes.

For internal points, two cases of I.P. = 0, 9 are considered and the results are presented in each mode (Table 2(c)). In this example, internal points can not help the results and I.P. = 0 is selected.

After completion of RBF adaptive procedure, dynamic analysis is performed for a harmonic unit transversal motion of beam's base. The amplitude of the harmonic displacement Uy at the center of

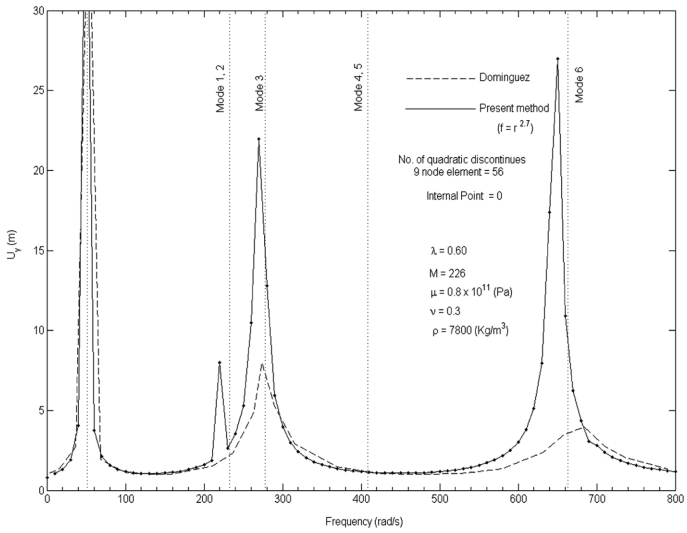

Fig. 8 Amplitude of the displacement at the center of beam's free end

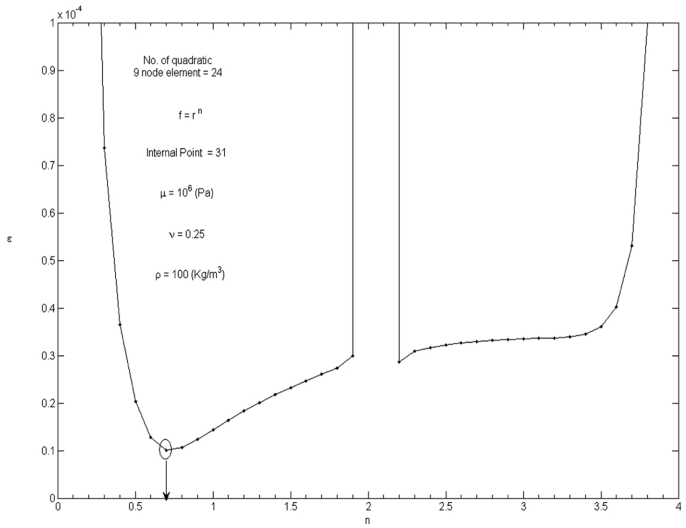

Fig. 9 Adaptive n selection in radial basis function $f = r^n$ for the sphere

beam's free end (Fig. 8) shows good agreement of adaptive procedure with result of Dominguez (1992).

Example. 3- An elastic sphere of radius r = 6 (m) is solved by the RBF adaptive DR/BEM. The material properties are as follows:

Shear modulus $\mu = 10^6$ (Pa),

Poisson's ratio $\nu = 0.25$,

Mass density $\rho = 100$ (Kg/m^3)

The sphere is discretized to 24 nine-node-quadratic elements (Fig. 2d). The eigenfrequencies of

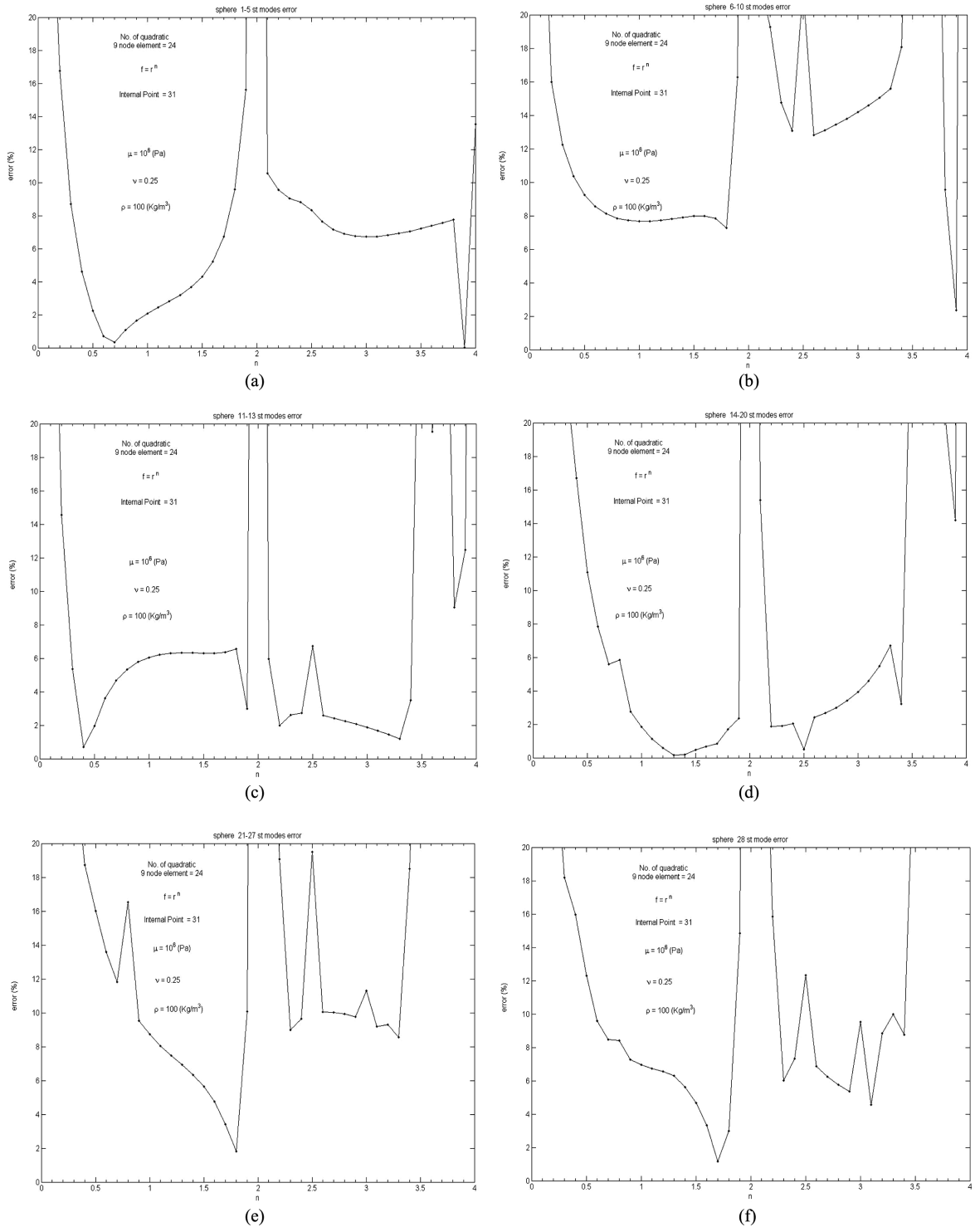

Fig. 10(a)-(f) Eigenfrequencies error of the sphere

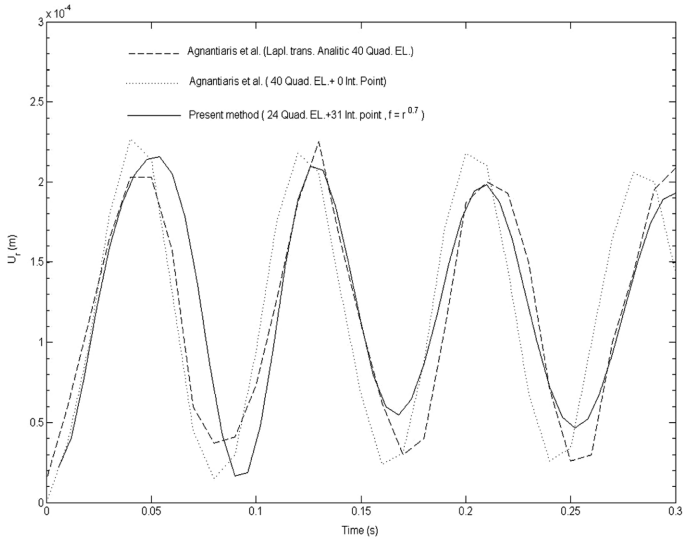

Fig. 11 Time History of the radial displacement on the surface of the sphere

Table 3(a) Normalized eigenfrequencies of the sphere (24El., $f = r^{0.7}$, $M = 98$)

Mode	ω_i^* (Type)	(I.P. = 0) $\hat{\omega}_i^*$ e_i (%)	(I.P. = 13) $\hat{\omega}_i^*$ e_i (%)	(I.P. = 31) $\hat{\omega}_i^*$ e_i (%)
1-5	2.501 (Torsional)	2.492 (0.35)	2.493 (0.34)	2.493 (0.33)
6-10	2.640 (Spheroidal)	2.908 (10.34)	2.881 (9.13)	2.854 (8.12)
11-13	3.424 (Spheroidal)	3.396 (0.81)	3.343 (2.36)	3.264 (4.66)
14-20	3.865 (Torsional)	4.090 (5.81)	4.086 (5.73)	4.081 (5.59)
21-27	3.916 (Spheroidal)	4.413 (12.68)	4.399 (12.32)	4.379 (11.83)
28	4.440 (Spheroidal)	4.894 (10.32)	4.894 (10.23)	4.816 (8.48)

the sphere are normalized with the expression $\omega^* = \omega r\sqrt{\rho/\mu}$.

For models consisting of only continuous elements, the geometric and collocation nodes are the same and M can be easily selected equal to all geometric boundary nodes.

With $M = 98$, the specification of the RBF $f = r^n$ for $0 < n < 4.0$ are as follows:

The result of RBF adaptivity in this example (Fig. 9) shows that the interval of $2.5 < n < 3.1$ have agreeable results and $n_{opt.}$ is equal to 0.7. Checking the adaptivity results, the errors of first 28 natural frequencies are derived (Figs. 10a-f) based on analytic results calculated by Leissa and Zhang (1983). They show that each mode has own $n_{opt.}$ but $n = 0.7$ has acceptable errors in all first 28 modes.

For internal points, four cases of internal point = 0, 7, 13, 31 are considered and the results are presented in each mode (Table 3(a)). Comparing the differences between four cases results, I.P. = 31 can be selected. As shown in Table 3(a) using 31 internal points improves the accuracy of sphere's eigenfrequencies in modes 1-10 & 14-28.

After completion of RBF adaptive procedure, the sphere is subjected to a suddenly applied uniform radial pressure $P = P_0H(t)$ where $P_0 = 100$ (Pa) and $H(t)$ is the Heaviside function. The time history of the radial displacement Ur is compared with that obtained by Agnantiaris *et al.* result with $f = 1 + r$. The time step used in Houbolt's time integration scheme is $\Delta t = 0.006$ (s) which is corresponding to $\beta = 0.51$. The results of the RBF adaptive DR/BEM are shown to be in close agreement with Agnantiaris *et al.* results. The reduction of required elements from 40 to 24 demonstrates the efficiency of the presented method.

5. Conclusions

A new adaptive dual reciprocity boundary element method for dynamic analysis of 3-D structures is presented. The adaptive method is based on finding the best approximation function of a radial basis function (RBF) group $f = r^n + c$. It helps us to reduce the error of expanding the displacement field which is necessary for dual reciprocity method. As the effect of augmentation parameter 'c' is negligible, the function can be reduced to $f = r^n$.

The following steps should be considered for implementation of RBF adaptivity:

1- Assignment of suitable RBFs number (M)

The RBFs number which equals to selected geometrical boundary points (M) directly is used in expansion of displacement field. The results show that the best selection of geometrical boundary points of models which is discretized with discontinuous elements, is using all geometrical element nodes of the model that usually is less than boundary nodes number. For a model which is discretized with continuous elements, maximum of M equal to $N + L$ is the best selection.

2- Assignment of parametric position of collocation nodes (λ) in discontinuous elements

3- Minimization of ε in sequence of 'n' and derivation of $n_{opt.}$

In this paper, searching for $n_{opt.}$ is limited to the interval $0.0 < n < 4.0$ that seems to be enough. The numerical examples show that each mode of natural frequencies has own $n_{opt.}$ but the optimum 'n' derived from RBF adaptivity has acceptable errors in all several first modes. Also, $n_{opt.}$ in all cases are located in one of two intervals $0.5 < n < 1.8$ and $2.3 < n < 3.7$

4- Assignment of internal points (I.P.)

Using some internal points can help results in case of coarse mesh but in a model with fine mesh, this may increase the error of natural frequencies. The internal points should be distributed in the structure as uniformly as possible.

After completion of RBF adaptive procedure, dynamic analysis with DR/BEM can more accurately be done. A harmonic forced vibration in frequency and a transient Heaviside loading in time domain are implemented to the examples and the results show the improvement of accuracy with respect to ordinary DR/BEM.

References

Agnantiaris, J.P., Polyzos, D. and Beskos, D.E. (1996), "Some studies on dual reciprocity BEM for elastodynamic analysis", *Comput. Mech*., **17**, 270-277.

Agnantiaris, J.P., Polyzos, D. and Beskos, D.E. (1998), "Three-dimensional structural vibration analysis by the Dual Reciprocity BEM", *Comput. Mech.,* **21**, 372-381.

Agnantiaris, J.P., Polyzos, D. and Beskos, D.E. (2001), "Free vibration analysis of non-axisymetric and axisymetric structures by the dual reciprocity BEM", *Eng. Anal. Bound. Elem*., **25**, 713-723.

Dominguez, J. (1992), *Boundary Elements in Dynamics.* Computational Mechanics Publications and Elsevier.

Golberg, M.A., Chen, C.S. and Karur, S.R. (1996), "Improved multiquadric approximation for partial differential equations", *Eng. Anal. Bound. Elem.,* **18**, 9-17.

Golberg, M.A., Chen, C.S., Bowman, H. and Power, H. (1998), "Some comments on the use of radial basis functions in the dual reciprocity method", *Comput. Mech*., **22**, 61-69.

Jumarchon, B. and Amini, S. (1999), "Towards a convergence analysis for the dual reciprocity method", In: Brebbia, C.A., Power, H., editors. Boundary Elements XXI. Southampton, Boston: WIT Press.

Leissa, A. and Zhang, Z. (1983), "Three-dimensional vibrations of the cantilever rectangular parallelepiped", *J. Acoust. Soc. Am.,***73**(6), 2013-2021.

Nardini, D. and Brebbia, C.A. (1982), "A new approach to free vibration analysis using boundary elements", In: Brebbia, C.A., editor. Boundary Element Methods in Engineering. Berlin: Springer, 313-326.

Partridge, P.W. (1997), "Approximation functions in the dual reciprocity method", *Bound. Elem. Commun.,* **8**, 1-4.

Partridge, P.W. (2000), "Towards criteria for selecting approximation functions in the Dual Reciprocity Method", *Eng. Anal. Bound. Elem*., **24**, 519-529.

Wang, H.C. and Banerjee, P.K. (1988), "Axisymmetric free-vibration problems by boundary element method", *J. Appl. Mech*., **55**, 437-442.

Wang, H.C. and Banerjee, P.K. (1990), "Free vibration of axisymmetric solids by BEM using particular integrals", *Int. J. Numer. Meth. Eng*., **29**, 985-1001.

Wilson, R.B., Miller, N.M. and Banerjee, P.K. (1990), "Free vibration analysis of three-dimensional solids by BEM", *Int. J. Numer. Meth. Eng.*, **29**, 1737-1757.

Zhao, Z. and Wang, X. (1999), "Error estimation and h adaptive boundary elements", *Eng. Anal. Bound. Elem*., **23**, 793-803.